We are IntechOpen,
the world's leading publisher of
Open Access books
Built by scientists, for scientists

6,300
Open access books available

170,000
International authors and editors

185M
Downloads

Our authors are among the

154
Countries delivered to

TOP 1%
most cited scientists

12.2%
Contributors from top 500 universities

CLARIVATE ANALYTICS
BOOK CITATION INDEX
INDEXED

WEB OF SCIENCE™

Selection of our books indexed in the Book Citation Index
in Web of Science™ Core Collection (BKCI)

Interested in publishing with us?
Contact book.department@intechopen.com

Numbers displayed above are based on latest data collected.
For more information visit www.intechopen.com

Chapter

Probabilistic Seismic Vulnerability and Loss Assessment of the Buildings in Mexico City

Alonso Gómez-Bernal, Antonio Romero Peña
and Jonathan de Anda Gil

Abstract

This article presents a seismic vulnerability and risk assessment of buildings in Mexico City. A probabilistic seismic hazard analysis (PSHA) was carried out, which allowed the definition of seismic hazard curves as well as uniform hazard spectra (UHS) for several seismic zones. The seismic hazard includes the effects of all seismic sources located in an influence area with a radius of 500 km. Attenuation relationships were selected with basis in attenuation models of events affecting the areas of Central Mexico and were complemented by our own functions that include local soil effects. Already established the sources and attenuation functions, the seismic hazard is quantified throughout UHS, which calculated using a return period Tr = 100 years. For the vulnerability assessment, fragility curves were defined. Two groups of fragility curves were studied, the first for the first for buildings built before 1985, and the second for buildings built after 1985. In the first case, static nonlinear analyzes of selected buildings were performed to define the capacity spectra. In the second case, the capacity spectra were defined from design spectra of the Mexico City Building Code. The results showed a very good correlation with the seismic demands of the 2017 earthquake.

Keywords: Mexico earthquakes, vulnerability in Mexico City, seismic risk in Mexico City, seismic hazard in México

1. Introduction

1.1 The seismic vulnerability assessment

The ability to assess the vulnerability of residential infrastructure to earthquake damage is undoubtedly one of the most important challenges facing structural engineers. Two methods are typically used to predict earthquake damage: nonlinear finite element analysis (FE) and seismic vulnerability curves. Nonlinear FE analysis is particularly applicable when a detailed damage estimate is required only for a small

number of structures. However, if an estimate is required for the many structures, the process becomes slow and inefficient. Seismic vulnerability curves provide a more efficient method for predicting damage to a class of similar structures. These curves often relate strong ground motion and structural properties to damage.

Vulnerability curves are generally constructed from statistical analyses of historical field data, as example Ref. [1], or analytically simulated data, as Ref. [2]. However, the number of parameters considered when creating vulnerability curves is usually very limited. Research on widespread methods of damage prediction has been scarce. Notable examples include Ref. [3, 4] who used discriminatory analysis to predict the damage to buildings in a classification of two or three damage degrees (DD). Vulnerability studies have recently been conducted using artificial neural networks [5], where the soil movement intensity parameter is correlated with the damage states of type structures, for large-scale risk analysis. In a vulnerability study [6], defined sets of single-degree freedom oscillators and a series of ground motion records using nonlinear time history analysis, and the resulting damage distributions were used to derive sets of fragility functions.

1.2 The two catastrophic earthquakes of September 19: 1985 and 2017

Many of the seriously damaged buildings during the September 19, 2017, Earthquake (M = 7.1) were medium-height buildings (4–10 stories), with natural periods ranging between 0.7 to 1.4 sec, located in the Lake-bed zone. **Figure 1a** shows the location of the buildings that suffered the greatest damage caused by the 2017
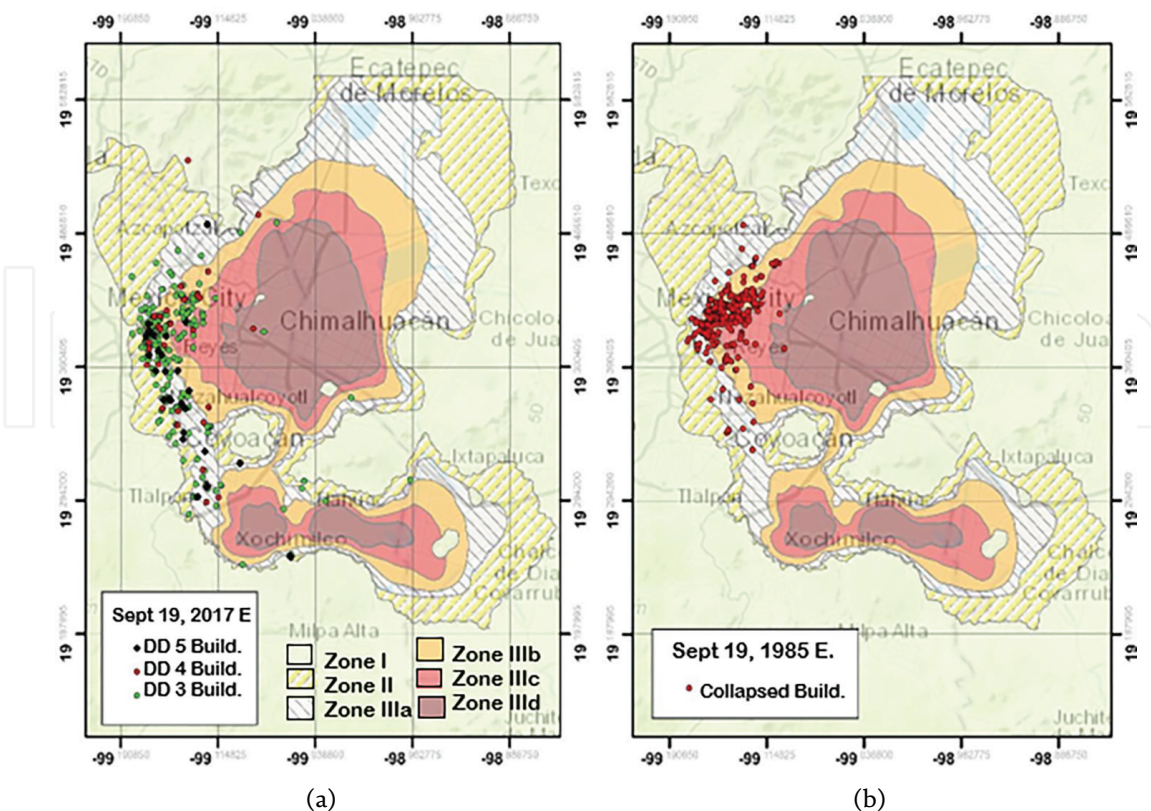

Figure 1.
(a) Damaged buildings due to the September 19, 2017, Earthquake: Damage Degree 5 (DD5), Damage Degree 4 (DD4), Damage Degree 3(DD3). (b) Collapsed buildings during September 19, 1985, Earthquake.

earthquake (DD3, DD4, and DD5), while **Figure 1b** shows the location of the collapsed buildings (DD5) for the September 19, 1985, Michoacan Earthquake (M = 8.1); As can be seen, these damages occurred in the same area of the Valley of Mexico for both earthquakes. One of the most vulnerable typologies corresponds to buildings structured with columns of reinforced concrete without girders and supporting a waffle slab, which was built before the September 19, 1985, Earthquake. A complete information statistic of damaged buildings during September 19, 2017, Earthquake, could be founded for example in Ref. [7, 8]. Among the principal causes of buildings damaged were, a) lack of seismic strength; b) structural irregularities, in this case, most configuration problems were associated with the contribution of no-structural elements to the building response, especially in corner buildings; and c) tilting and foundation problems.

This study focuses on the vulnerability assessment of two groups of buildings, the first the structures built before 1985 when the 1976 Mexican Building Code [9] was applicable, and the second includes those built after that date.

2. Methodology

With the purpose of assigning structural vulnerability to the building population of México City, it is necessary to apply an analytical methodology for assessing the seismic response of a class of buildings, which is combined with a damage model in order to derive sets of fragility functions for different levels of seismic behavior. The seismic vulnerability assessment developed in this paper focuses mainly on the HAZUS methodology [10] and RISK-EU [11], which has been adapted for damaged buildings in Mexico City during the September 19, 2017, earthquake.

The methodology developed consists in general of the following steps: (1) seismic hazard assessment for Mexico City, using a probabilistic procedure, for the calculation of the uniform hazard spectra (UHS). (2) Definition of the capacity curves of structural systems, in this case, data from damaged buildings representative of the most vulnerable typology were used for the September 19, 1985 and 2017 earthquake, but analytical models representative of other common typologies of structures built after 1985 were also used; (3) Definition of the damage criteria adopted and development of capacity spectrums; (4) Estimation of the medium capacity curves, which are represented in their bilinear form to define the damage thresholds and thereby build the fragility curves and their damage probability matrices; (5) calculation of overall damage of the structure analytically. The fragility curves resulting from this study were calibrated with the event of September 19, 2017.

3. Seismic hazard analysis

3.1 Probabilistic seismic hazard analysis PSHA

The seismic hazard for Mexico City was developed with a probabilistic seismic hazard analysis (PSHA). The PSHA use of probabilistic concepts has allowed uncertainties in the location, size, and rate of recurrence of earthquakes and in the variation of ground motion characteristics with earthquake size and location to be explicitly considered in the evaluation of seismic hazards [12]. In this study, the seismic hazard

settings were defined, using uniform hazard spectra (UHS) and seismic parameters. Three ground motion prediction equations (GMPEs) were revised and used, and a disaggregation study was performed. Site effects estimations were included in the prediction equations. UHS was established for both firm and soft soils for Mexico City. Finally, the computed seismic parameters were compared to those for the seismic design guidelines for Mexico City, and we found out that our UHS captured better the seismic settings.

The model characterization for the earthquake occurrence, the seismic sources, the magnitude-recurrence, and the attenuation laws are statistically evaluated (see for example [13, 14]). The probabilistic seismic hazard analysis is characterized by four stages [12]), these stages can be summarized as 1) identification and characterization of seismic sources, historical descriptions, seismic catalogs, isoseismal maps, and instrumental information; 2) Definition of recurrence relationships, it is necessary to ensure that data is homogeneous, independent, and complete (events with M > 5). The recurrence ratio, which specifies the average rate at which an earthquake of some size will be exceeded, is used to characterize the seismicity of each source zone. Gutenberg's law was used. 3) Definition of predictive relationships. 4) development of seismic hazard curves, for which, the uncertainties in earthquake location, earthquake size, and ground motion parameter prediction are combined to obtain the probability that the ground motion parameter will be exceeded during a particular time period.

The equation used to assess the seismic hazard according to the classical methodology is:

$$\lambda(y > Y) = \sum_{i=1}^{N} \lambda_i(y > Y) = \sum_{i=1}^{N} \upsilon_i \iiint P_i\left[y > Y | m, r, \epsilon\right] f_{Mi}(m)\ f_{Ri}(r)\ f_{\epsilon i}(\epsilon)\ dm\ dr\ d\epsilon$$

$$(1)$$

where $\lambda(y > Y)$ is the annual rate of exceedance of the level of ground motion Y, due to the occurrence of earthquakes in the N seismic sources, which is equal to the sum of the annual rates of exceedance in each source zone $\lambda i(y > Y)$, the same ones that present an annual rate of earthquakes vi; the term $Pi[y > Y | m, r, \epsilon]$ gives the probability of conditional exceedance to the trio of variables m, r, and ϵ representing magnitude, distance, and epsilon; fMi $(m)fRi$ (r) $f\epsilon i(\epsilon)$ are the probability density functions of magnitude, distance, and epsilon [15].

3.2 Hazard curves and UHS for Mexico City

The identification of the seismotectonic regions is one of the most important stages in the seismic hazard procedure, in order to understand the seismicity of each region that is the characteristics of earthquake occurrence and to identify whether a source, close to the site, is active or not, as well as the definition failure mechanisms. We considered two types of seismic sources capable of producing earthquakes in Central Mexico: faults and areas. Seismic sources are modeled in a seismic hazard assessment with their geometric and recurrence characteristics.

Of the thirteen segments or gaps characteristic of the country, six faults were selected and characterized in this study since the interplate sources that are within a radius of influence of 500 km were analyzed. **Figure 2a** shows the six fault segments
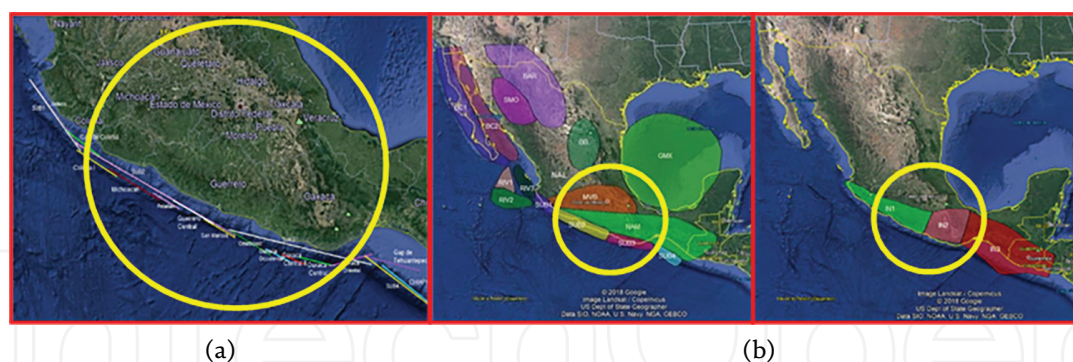
Figure 2.
(Left) Faults along the Pacific Coast [11]. (Center and Right) Seismic sources type Area affecting Mexico City [12].

described by Ref. [16] that affect the Central Mexico segment are, Oaxaca Este (OX-E), Oaxaca Central (OX-CI and OX-CII), Oaxaca Oeste (OX-O), Ometepec (OX-M), Acapulco-San Marcos (AC-SM), Guerrero Central (GC), Petatlán (PE), and Michoacán (MI). We have considered an area where earthquakes might occur, with a radius 500 km (red circle in **Figure 2b**), these areas were selected according to the faults described by [17].

Part right and center of **Figure 2** illustrate the 19 seismic sources type-Area parameters, which describe the area where seismic events are presented; these parameters can be consulted in Ref. [18], namely, the focal depth, the activity rate or number of events per year that exceed the minimum magnitude for each source, the parameters of the Richter model, and the estimated minimum and maximum seismic moment magnitudes (M_w).

We use two sets of spectral acceleration attenuation (SA) functions; the first group includes classical functions [19–23] developed with a global database, while for the second group, we use attenuation relations developed by us [18] of strong ground motion recorded in Mexico City with M > 6.0, in both groups we considered interplate and intraslab seismic sources.

For the Hazard assessment the probabilistic procedure described above was used. For the calculation of the hazard curves and the uniform hazard spectra, UHS, we used the EZ-FRISK package [24]. **Figure 3** shows the seismic hazard curves in Zone I, Zone II, and Zone IIIb, as an example of the several sites studied. In **Figure 3**, uniform hazard spectra (UHS) are included for six return periods, namely, 40, 100, 250, 475, 975, and 2475 years, which represent, respectively, 68%, 39.3%, 20% 10%, 5%, and 2% exceedance. Probability of occurring in 50 years. These spectra show the highest spectral acceleration values in Mexico City, ranging from 0.8 g to 1.05 g, indicating a high hazard in Zone III for intraplate and interplate events.

When the shape of the spectral ordinates in sites of Mexico City obtained with our functions are compared with other relationships, we observed significant differences in periods ranging between 1 and 2 s, mainly due to the incorporation of a regression model, which considers local effects, and as seen in **Figure 3**, it provides good esti-mates of the spectral accelerations. UHS from sites in Zone I, Zone II, and Zone IIIb cover a larger range of periods.

As an example, **Figure 4** present the displacement spectra in Zone IIIb calculated using synthetic accelerograms, which were defined from the UHS assuming a return
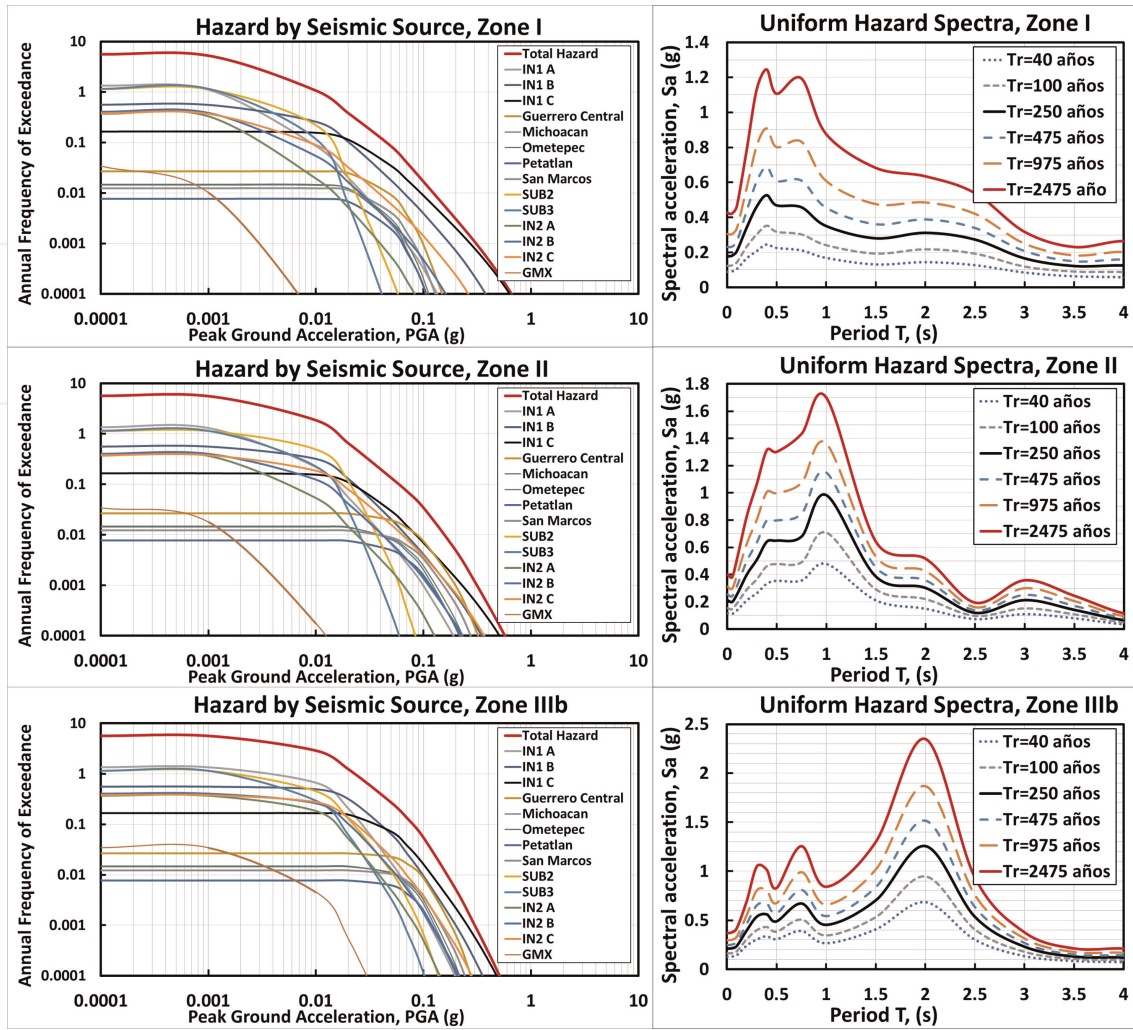
Figure 3.
Left: Hazard curves obtained in Zone I, Zone II, and Zone IIIb and Right: the corresponding uniform hazard spectra (UHS) for several return periods.
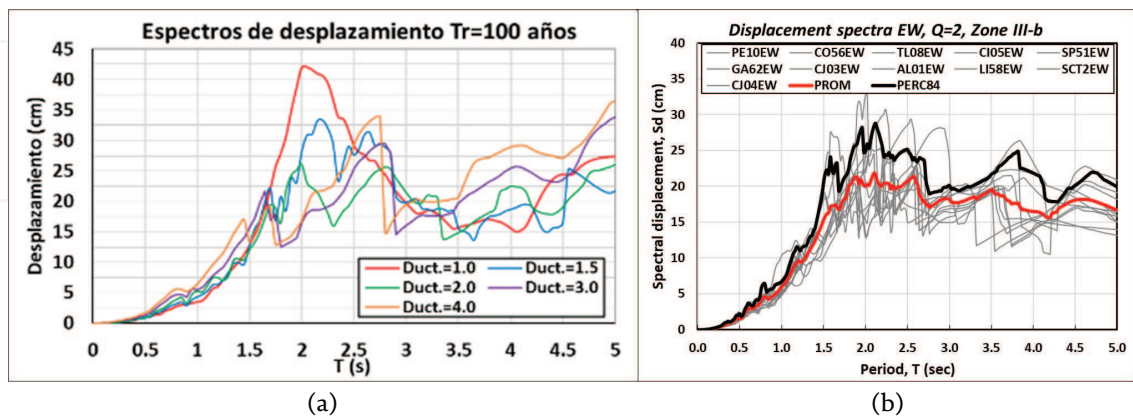

Figure 4.
Left: Displacement spectra in Zone IIIb calculated from synthetic records for UHS and a return period
Tr = 100 years Right: Displacement spectra at stations in Zone IIIb due to September 19, 2017, Earthquake.

period Tr = 100 years. The right part of **Figure 4** is compared this result with the displacement spectra of stations located in Zone IIIb due to the September 19, 2017, earthquake.

4. Numerical models

4.1 Buildings characteristics

The identification and selection of structural systems to be studied typical of an area is initially carried out. In this case, five buildings of a very common typology in Mexico City were selected, which has been very vulnerable to the two earthquakes of September 19 (1985 and 2017), and other seismic events.

With the purpose of studying existing buildings constructed before 1985 in Mexico City, the five medium-rise buildings damaged by the 2017 earthquake were analyzed (**Figure 5**). These buildings were built on reinforced concrete columns and reticular waffle slabs, four of them are in the Benito Juárez Sector and one more in the Cuauhtémoc Sector. All buildings are for housing use and are classified within group B according to the México City Building Code [8]. **Table 1** summarizes the main characteristics of the five buildings, including the EME-98 classification of the damage degree assigned after the 2017 earthquake.

Once the structures to be studied have been modeled, the main parameters to be considered are defined. The main function of this variation is to obtain a standard deviation from the potential capabilities of each of the analyzed models and consider them within their vulnerability assessment. The definition of the damage thresholds was made according to **Table 2**.

These buildings have long rectangular plants as shown in **Figure 3**, as can be seen, with the exception of the SE2–7 N building, the structures exceed or are equal to the value of 2.5, which is a limit value suggested in all structural recommendations because when exceeded, it has been observed that the structural response can be amplified and the torsional effects can also be increased, in addition, all these structures have no girders and the slab have relatively low depths, which generates flexible

Key	Age	Stories	Height	Bay	L_1	L_2	Zone	d slab	Cols	L_1/L_2	DD
SE2–5 N	1977	5	13.80	2	14.62	7.31	IIIa	35	70x35	2.4	DD2
SE2–7 N	1982	7	18.90	3	13.50	3.40	IIIa	35	55x45	1.5	DD3
SE2–8 N	1983	8	22.25	3	15.75	5.25	IIIa	25	65x35	5.4	DD3
SE2–10 N	1978	10	26.0	1	7.68	7.68	IIIb	35	50x80	3.3	DD3
SE2–12 N	1980	12	32.4	2	13.00	6.33	IIIa	35	145x40	2.5	DD3

Table 1.
General characteristics of the selected buildings [25].

Damage degree	ID	Damage threshold
No damage	ND	—
Sligth	DL	Sd1 = 0.7Dy
Moderate	DM	Sd2 = Dy
Severe	DS	Sd3 = Dy+0.25(Du-Dy)
Completo	DC	Sd4 = Du

Table 2.
Definition of damage threshold.

frames away from being shear systems. Another factor that increases the vulnerability of these buildings is the unfavorable orientation of the columns with their minor axis on the short side.

4.2 Capacity curves

For all buildings studied, a nonlinear static analysis (Pushover) was performed using the SAP program to define the capacity curves of each model. The structural configuration and considered loads of buildings are defined in Ref. [25]. The different capacity curves of the models analyzed are presented in part left of **Figure 5**. According to the results, it is possible to note that the model of the structure SE2–10 N is the one that provides the least resistant capacity since its last capacity is presented when a basal shear of Vu = 25.6 Ton occurs, with a roof displacement of 27 cm, while the strongest structure corresponds to the model SE2–7 N, where its basal shear is Vu = 60.31 Ton, with a roof displacement of 31 cm.

To obtain the ductility, μ, of the system it is necessary to represent the capacity curve in its bilinear form, which is obtained by defining the yield point and the ultimate capacity point of the structure. The procedure used in this study corresponds to that proposed by FEMA 356 [14], which is based on matching the energy dissipated by the structure defined by the area under the actual curve with the dissipated energy of the idealized curve. **Table 2** presents some of the most important points that define the capacity curves obtained in their bilinear form.

4.3 Capacity spectra

To compare the seismic demand with the capacity of the structure, it is necessary to transform the result of pushover to another curve that relates the spectral displacement *Sd* with the spectral acceleration *Sa*. This transformation is known as the capacity spectrum and develops by applying the dynamic characteristics of the fundamental mode. The capacity spectrum is determined using the following equations:

$$Sd_j = \frac{Dt_j}{\gamma_M \varphi_{t1}} \tag{2}$$

$$Sa_j = \frac{V_j}{M_T \alpha} \tag{3}$$

where:
D_{tj} = displacement of each point of the capacity curve [cm].
V_j = shear of each point of the capacity curve [Ton].
γ_M = participation factor of the first mode.
α = effective mass coefficient of the basal shear of the first mode.
φ_{t1} = maximum top amplitude of the structure associated with the first mode.
M_T = total mass of the structure.
The capacity spectrum is defined by two main points: the ultimate capacity point (UC) and the yield capacity point (YC), which are expressed as follows:

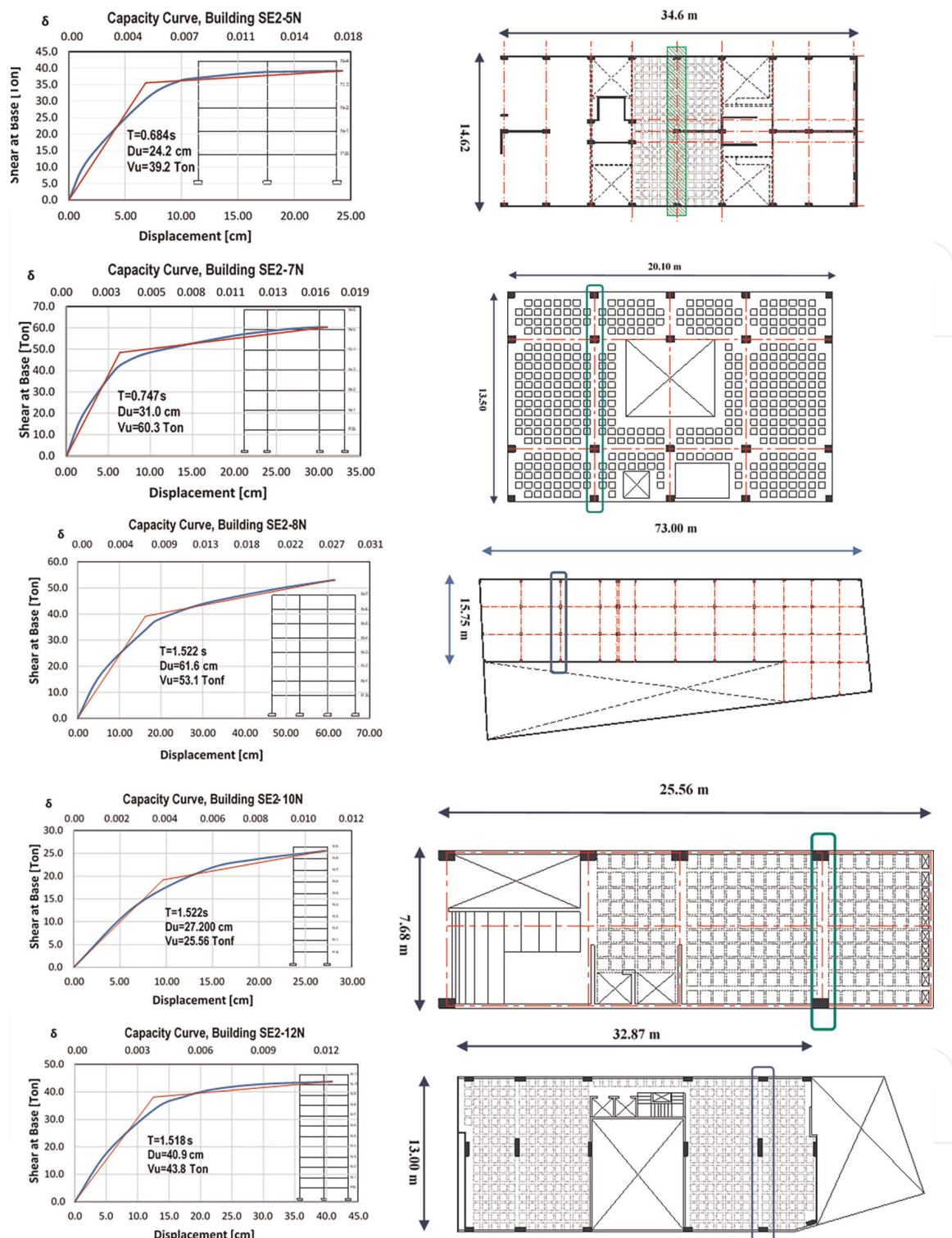$$YC\left[A_y = S_{ay} = \frac{C_s SR}{\alpha_1}; Dy = S_{dy}\right] \tag{4}$$

Figure 5.
Right: Structural plants of the buildings studied. SE2–5 N, SE2–7 N, SE2–8 N, SE2–10 N, SE2–12 N. Left: The corresponding capacity curves of the studied buildings.

$$UC\left[A_u = S_{au} = \lambda A_y; D_u = S_{du}\right] \tag{5}$$

where C_s represents the design seismic coefficient. This value is calculated using Eq. (4), and an approximate overstrength of the buildings analyzed is obtained.
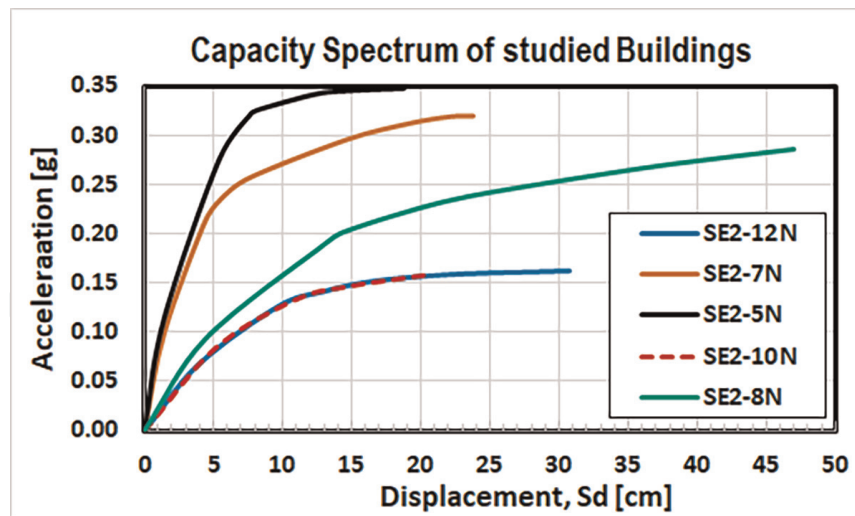
Figure 6.
*Capacity spectrum, derived from the capacity curves of **Figure 5** for the five selected buildings.*
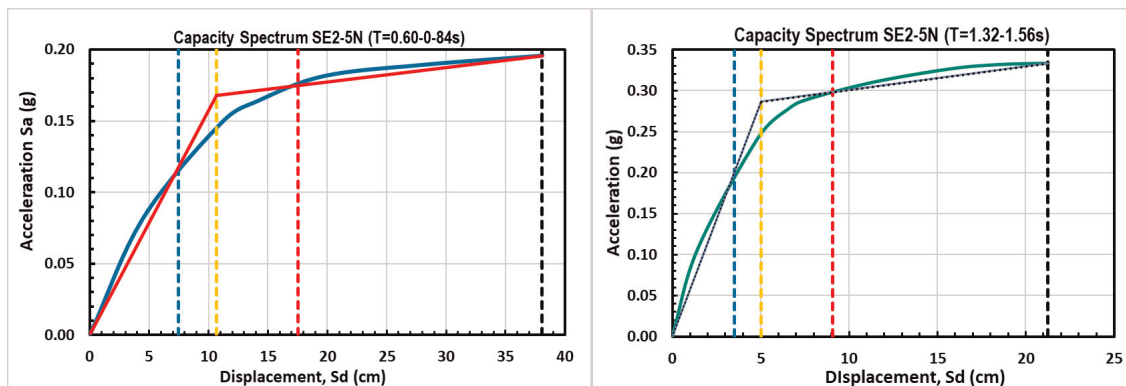

Figure 7.
Mean capacity spectra for buildings with short and long periods; damage thresholds are indicated in each case (DD2 to DD5).

As part of the methodology used in this work, the buildings analyzed were divided into two groups. Firstly, based on the characteristics and properties of each one of these structures, the dispersion of the capacity curves is greater among the buildings with five to seven levels and those from eight to 12 levels (**Figure 6**). Secondly, it is desired to reduce the uncertainty that exists due to this difference since there are only five buildings analyzed. For this reason, two mean capacity curves have been calculated, one for buildings with short periods and another for buildings with periods longer than 1 sec (**Figure 7**). This division by periods is also useful and of great interest since it allows classifying the type of buildings that were most vulnerable to the earthquake of September 19, 2017. Capacity spectra of **Figure 7** show the bilinear representation. From these capacity curves in their bilinear form, the thresholds were defined, of damage for each type (**Table 2**).

5. Fragility curves and damage probability matrices

Fragility curves are a graphical representation of the cumulative distribution function of the probability of reaching or exceeding a specific state of damage, given a

Damage degree	ID	Damage (%)	FDC (%)	SE2–5		SE2–7		SE2–8		SE2–10		SE2–12	
				Prob (%)	D. I.	Prob (%)	D.I.	Prob (%)	D.I.	Prob (%)	D.I.	Prob (%)	D.I.
No damage	DD1	0–10	5	45.7	2.3	21.4	1.1	4.6	0.2	0.4	0.0	5.5	0.3
Sligth	DD2	10–30	20	36.5	5.9	41.0	8.2	29.0	5.8	11.3	2.3	30.6	6.1
Moderate	DD3	30–60	45	11.4	8.2	25.4	11.4	43.2	19.4	41.0	18.5	42.5	19.1
Heavy	DD4	60–90	75	5.9	4.4	11.0	8.3	19.2	14.4	37.2	27.9	17.9	13.4
Complete	DD5	90–100	100	0.5	0.5	1.1	1.1	4.0	4.0	10.0	10.0	3.6	3.6
			Σ		20		30		44		59		43

Damage index, D.I. = Prob x FDC

Table 3.
Damage degree and damage index in the five buildings.

structural response, to a given seismic action. The HAZUS methodology [11] defines fragility curves and a lognormal probability distribution defined by the following equation.

$$P[ED \geq ED_i] = \Phi\left[\frac{1}{\beta_{ED}} \ln\left(\frac{Sd}{\overline{Sd}_{ED}}\right)\right] \qquad (6)$$

where $\overline{Sd}_{ED}$ is the average spectral displacement for which the probability of exceedance is 50%; $\boldsymbol{\beta_{ED}}$ is the standard deviation of the natural logarithm of spectral displacement, $\boldsymbol{\Phi}$ is the cumulative standard normal distribution function, and $\boldsymbol{S_d}$ is the spectral displacement.

In this methodology, each fragility curve is defined by the average spectral displacement value corresponding to the threshold of each damage state defined in **Table 2**. The standard deviation was calculated using two methods and adjusted to the mean of both. The first method obtains the standard deviation using the different actual capacity curves, while the second method adjusts the fragility curves with a discrete probability distribution (**Table 3**).

5.1 Fragility curves for buildings constructed before 1985

The fragility curves calculated for the first type of buildings, that is, between five and seven stories (with vibration periods between 0.60 and 0.86 s), are presented on the left side of **Figure 8**. In addition, the values of the spectral displacements S$_d$ corresponding to the hazard spectrum for a return period Tr = 100 years in Zone IIIb, are included in each curve (see **Figure 4**). **Table 3** indicates the average damage factors and the central damage factor, FDC, for each case.

5.2 Fragility curves for buildings constructed after 1985

In order to include buildings built with recent building regulations, theoretical models of buildings were included from the design spectra of the 2004 Complementary Technical Standards for Design by Sism (GDF, 2004). **Figure 9** shows the
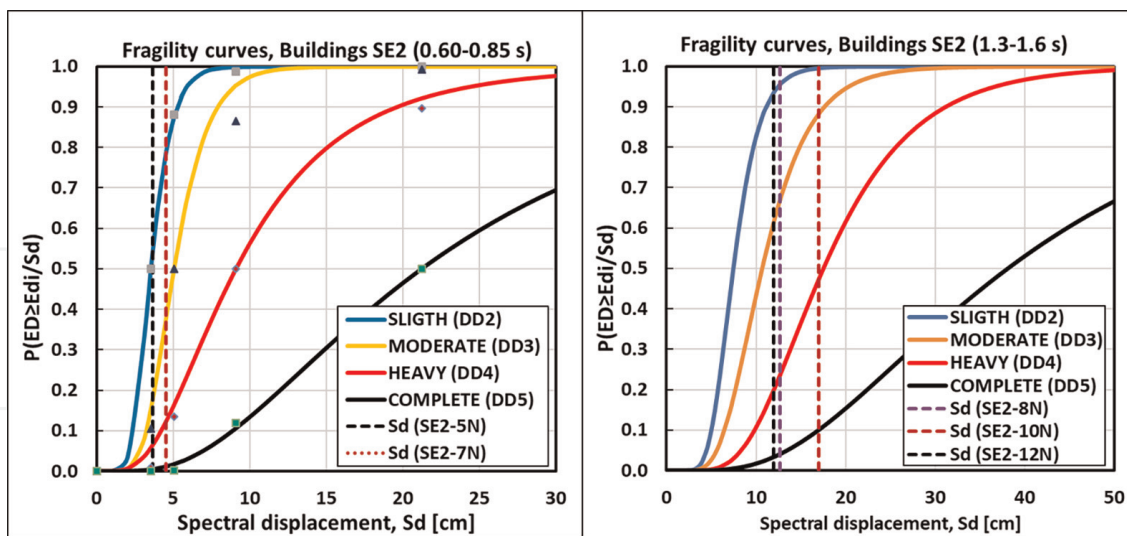
Figure 8.
Fragility curves that are indicated by dashed lines the Sd displacements for each building according to its period calculated assuming a return period Tr = 100 years.
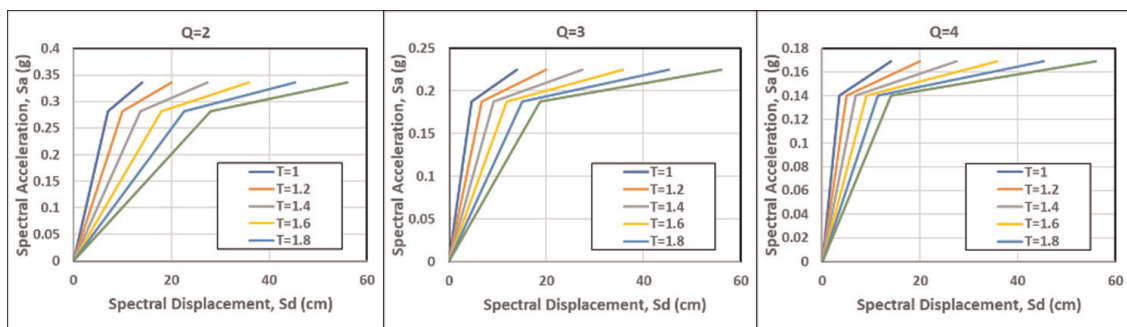

Figure 9.
Capacity spectra obtained from NTCS2004 [8] design spectra for Zone IIIb in Mexico City and using an overstrength factor of 1.5.

capacity spectra determined for three ductility reduction factors, Q = 2, Q = 3, and Q = 4, for structures built in Zone IIIb, and an overstrength factor of 1.5. These spectra are the basis for determining the fragility curves in **Figure 10**, following the same procedure used earlier. Fragility curves were calculated for six structural models with periods between 1.0 s and 2.0 s, with intervals of 0.2 s.

Figure 4b shows the displacement response spectra for 5% of critical damping at eleven stations in Mexico City's zone IIIb of September 19, 2017, which were calculated for elastic models and for models with ductility equal to two (Q-2). They are also indicated in the same **Figure 4**, the average or average response spectra and the spectrum corresponding to the 84% percentile, for all cases. It is important to note that there is little dispersion between the spectra of the different stations for displacement spectra, compared to acceleration response spectra.

In order to calibrate the fragility curves in **Figure 10**, the spectral displacement, Sd, for the return period Tr = 100 years (**Figure 4a**) associated with each natural period, is included in each of the six boxes. It can see that, in general, there is very good correlation with the behavior of the buildings of this group (built after 1985), observed during the 19 September 2017 earthquake.
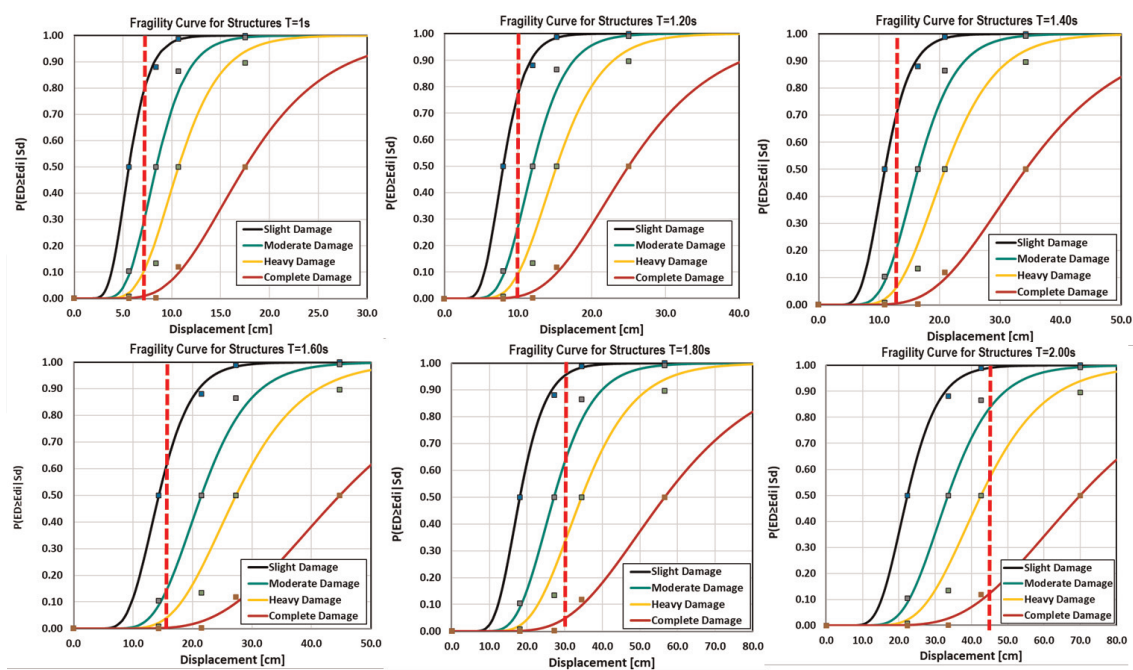
Figure 10.
Fragility curves for buildings using a coefficient of Q = 2 and with fundamental periods of 1.0, 1.2, 1.4, 1.6, 1.8, and 2.0 s.

6. Conclusions

In the first part of this article, a probabilistic seismic hazard analysis (PSHA) was carried out, which allowed the definition of seismic hazard curves as well as uniform hazard spectra for each of the six seismic zones of Mexico City; in this analysis, the seismogenic origin of the earthquakes was considered, that is, interplate or intraslab origin.

In the second part, the fragility curves that are the basis for establishing the damage index of buildings for a specific scenario were defined. Two groups of fragility curves were defined, the first for buildings built before 1985 and the second for buildings built after 1985. In the first case, nonlinear static analyzes (Pushover) of five buildings, which were performed to define the capacity curves and later the capacity spectra elements, were necessary to estimate the fragility curves. In the second case, the capacity spectra were directly defined from the design spectra of the Mexico City Building Regulations.

For the study of buildings built before 1985, five buildings were selected as representatives of this group, which have a structural system of columns of reinforced concrete with a waffle slab, and were damaged by the earthquake of September 19, 2017.

With the purpose to assign the vulnerability of residential buildings in Mexico City, the fragility curves of buildings built before 1985 were defined, which have a structural system of reinforced concrete columns with a lightened flat slab and which were damaged by the earthquake of September 19, 2017.

The findings of the probabilistic seismic hazard and probabilistic vulnerability analysis resulted in the following conclusions:

1. Uniform hazard spectra, UHS, were computed for return periods of 50, 100, 475, 975, and 2475 years. Specific attenuation relationships were developed for

Mexico City that directly includes local effects; in addition, to complement the study, classical predictive functions were used.

2. With the capacity curves of the buildings, their expected design ductility and overstrength were estimated. It was found that the average overstrength used for this type of structure (buildings built before 1985) is approximately 1.50.

3. With the uniform hazard spectra, displacement demands were defined for some return period, in this article a return period of 250 years was selected. These demands were combined with the capacity curves to obtain the percentages of damage expected for each degree of damage, and thus determine the damage index of the building.

4. The most vulnerable building due to the 19S-2017 earthquake was the 10-story building (SE2–10 N), which has an elongated floor plan with a B/A = 3.33 ratio, in addition to having only one span. This structure was assigned a damage degree due to the earthquake of 45%, while with the analytical method carried out, a global damage index of 59% was found, in both cases, it corresponds to a damage degree of 3 (DD3), or moderate damage.

5. On the other hand, the least vulnerable building turned out to be the 5-story one (SE2–5 N), since in the evaluation of the building a percentage of damage of 25% was assigned, while with the analytical method based on the fragility curves, a global damage index of 20% was determined, both cases correspond to damage degree of 2 (DD2), or slight damage.

6. For the estimation of the fragility of the buildings built with construction regulations after 1985, theoretical models of buildings were included based on the design spectra of the Mexican Construction Code, 2004. Capacity spectra were calculated for structure models in Zone IIIb; overstrength factor of 1.5 and a reduction factor of Q = 2 were used. When the results are compared with the spectral displacements registered by the 2017 earthquake, it can be verified that, in general, there is a very good correlation between results and observations.

7. In conclusion, the methodology used in this work shows that quite reasonable results are obtained, even though data from only a few buildings have been used; however, the buildings used in this work, which were damaged by the 2017 earthquake, are representative of hundreds of existing buildings in Mexico City. Besides, the study was complemented by the parametric study of the second part.

Author details

Alonso Gómez-Bernal*, Antonio Romero Peña and Jonathan de Anda Gil
Universidad Autónoma Metropolitana, Azcapotzalco, México City, Mexico

*Address all correspondence to: agb@azc.uam.mx

IntechOpen

References

[1] Hassan AF, Sozen MA. Seismic vulnerability assessment of low-rise buildings in regions with infrequent earthquakes. ACI Structural Journal. 1997;**94**(1):31-39

[2] Lang K, Bachmann H. On the seismic vulnerability of existing buildings: A case study of the City of Basel. Earthquake Spectra. 2004;**20**(1):43-66

[3] Yücemen MS, Özcebe G, Pay AC. Prediction of potential damage due to severe earthquakes. Structural Safety. 2004;**26**(3):349-366

[4] Yakut A, Ozcebe G, Yucemen MS. Seismic vulnerability assessment using regional empirical data. Earthquake Engineering and Structural Dynamics. 2006;**35**(10):1187-1202

[5] Lautour OR, Omenzetter P. Prediction of seismic-induced structural damage using artificial neural networks. Engineering Structures. 2009;**31**(2): 600-606. DOI: 10.1016/j. engstruct.2008.11.010

[6] Villar-Vega M, Silva V, Crowley H, Yepes C, Tarque N, Acevedo AB, et al. Development of a fragility model for the residential building stock in South America. Earthquake Spectra. 2017; **33**(2):581-604

[7] Gómez Bernal A, Arellano E, González O, y Juárez, H. Características, causas, y consecuencias de los daños debidos al sismo del 19 de septiembre de 2017 (M=7.1) en México. In: XII Congreso Chileno de Sismología e Ingeniería Sísmica. Asociación Chilena de Sismología e Ingeniería Antisísmica; ACHISINA, Chile, 2019

[8] Roeslin S, Ma Q, Juárez GH, Gómez BA, Wicker J, Wotherspoon L. A machine learning damage prediction model for the 2017 Puebla-Morelos, Mexico, earthquake. Earthquake Spectra. 2020;**36**(2_suppl):314-339. DOI: 10.1177/ 8755293020936714

[9] Gobierno del Distrito Federal, GDF. Normas Técnicas Complementarias para Diseño por Sismo. 2017. http://www. smie.org.mx/informacion-tecnica/ estados/reglamentos-construccion-ciudad-de-mexico.php

[10] Federal Emergency Management Agency FEMA. Multi-hazard loss estimation methodology. In: Earthquake Model. Washington, DC: Federal Emergency Management Agency FEMA and National Inst. of Building Sciences NIBS; 2003

[11] Federal Emergency Management Agency FEMA. HAZUS. Earthquake Loss Estimation Methodology. Washington, DC: Federal Emergency Management Agency and National Institute of Building Sciences; 1999

[12] Kramer SL. Geotechnical Earthquake Engineering. Civil Engineering and Engineering Mechanics Series. Vol. 1. Upper Saddle River, NJ: Prentice Hall; 1996

[13] Cornell CA. Engineering seismic risk analysis. Bulletin of the Seismological Society of America. 1968;**58**(5): 1583-1606

[14] McGuire RK. Seismic Hazard and Risk Analysis. Oakland: Earthquake Engineering Research Institute; 2004

[15] Aguiar R, Rivas A. Estudio Probabilístico de la Peligrosidad Sísmica de Ambato, en roca. Primera Edición: Microzonificación Sísmica de Ambato; 2018. pp. 1-22

[16] Nishenko SP, Singh SK. Conditional probabilities for the recurrence of large and great interpolate earthquakes along the Mexican Subduction Zone. Bulletin of the Seismatic Society of America. 1987;**77**:2094-2114

[17] Zúñiga R, Suárez G, Ordaz M, García-Acosta V. Peligro Sísmico en Latinoamérica y el Caribe. Mexico: Pan American Institute of Geography and History, IPGH; 1997

[18] Romero PA, Gómez BA, Arellano E. Evaluación de la Vulnerabilidad Sísmica de Edificios residenciales de la Ciudad de México. In: Memorias XXIII Congreso Nacional de Ingeniería Estructural. Sociedad Mexicana de Ingeniería Estructural SMIE, México; 2022

[19] Youngs RR, Chiou SJ, Silva WJ, Humphrey JR. Strong ground motion attenuation relationships for subduction zone earthquakes. Seismological Research Letters. 1997;**68**(1):58-73

[20] Abrahamson NA, Silva WJ, Kamai R. Summary of the ASK14 ground motion relation for active crustal regions. Earthquake Spectra. 2014;**30**(3): 1025-1055

[21] Atkinson GM, Boore DM. Empirical ground-motion relations for subduction-zone earthquakes and their application to Cascadia and other regions. Bulletin Seismatic Society of America. 2003; **93**(4):1703-1729

[22] Zhao JX, Zhang J, Asano A, Ohno Y, Oouchi T, Takahashi T, et al. Attenuation relations of strong ground motion in Japan using site classification based on predominant period. Bulletin Seismatic Society of America. 2006;**96**:3

[23] García D, Singh SK, Herráiz M, Ordaz M, Pacheco JF. Inslab earthquakes of Central Mexico: Peak ground-motion parameters and response spectra. Bulletin Seismatic Society of America. 2005;**95**:2272-2282

[24] Risk-Engineering. Ez-Frisk v.7.65. Golden, Colorado, USA: Manual Risk Engineering, Inc; 2022

[25] De Anda GJ. Vulnerabilidad sísmica de edificios construidos antes de 1985 en Ciudad de México a raíz del sismo del 19 de septiembre de 2017. Master's Thesis. Universidad Autónoma Metropolitana Azcapotzalco; 2020